Simplified Thermal Model of a Radial Flux Motor for Electric Vehicle Application

Moez Ayadi [1], Hana Kebaili [2], Mohamed Amine Fakhfakh [3], and Rafik Neji [4]

[1] *Department of Electrical Engineering, University of Sfax, moez.ayadi@enis.rnu.tn*
[2] *Department of Electrical Engineering, University of Sfax, hana@alinto.com*
[3] *Department of Electrical Engineering, University of Sfax, fakhfakhamine@yahoo.fr*
[4] *Department of Electrical Engineering, University of Sfax, rafik.neji@enis.rnu.tn*

Abstract

Heat transfer is the science that seeks to predict the energy transfer that takes place between material bodies as a result of a temperature difference. When designing an electric motor, the study of heat transfer is as important as electromagnetic and mechanical design. However, due to its three dimensional nature, it is generally considered to be more difficult than the prediction of the electromagnetic behaviour. For this reason, and the fact that the majority of designers have an electrical rather than mechanical background, thermal analysis is usually not given as much emphasis as the electromagnetic design. This paper presents the thermal model simplified of Permanent Magnet Synchronous Motor (PMSM) with radial flux for electric vehicle (EV) application. The thermal design technique used is the analytical lumped circuit. The equivalent circuit of the motor is implemented and simulated with MATLAB simulator. Simulations by Motor-CAD software were made in order to shows the accuracy of the proposed thermal model.

Keywords

thermal analysis, motor-CAD, PMSM, lumped circuit, flux radial

1. INTRODUCTION

Heat transfer is the science that seeks to predict the energy transfer that takes place between material bodies as a result of a temperature difference. The thermal management of the motor in a hybrid electric vehicle is important because the electrical insulation has a temperature limit, and also because the temperature of the motor affects its efficiency.

Indeed, the thermal modeling remains a very complex problem by the diversity of heat exchange which conditions the general behavior of the motor.

An accurate simulationon of the thermal behaviour of the motor within the power train is therefore an important aspect of designing an appropriate cooling system and strategy.

An approach consists in working out a thermal model of equivalent lumped circuit on the basis of analogy between electric magnitude and thermal magnitude: the power sources correspond to the heat sources, the currents with the heat flows and the potential differences to the differences in temperatures [Chaieb et al., 2010; Fakhfakh et al., 2008].

In this paper we prensent first the geometry of Permanent Magnet Synchronous Motor studied.

In the second part of the paper, an advanced thermal model simplified is proposed. This model represented by an equivalent electrical circuit which sweet well with circuit simulators where electrical behavior are studied.

In the third part of the paper, simulations by Motor-CAD and by thermal model are performed in order to validate the proposed advanced model. The final section concerns the motor behavior in the case of pulsed losses. Discussion about the thermal model accuracy is presented.

2. GEOMETRY OF THE MOTOR STUDIED

Figure 1 shows the geometry of the PMSM design used in this study. The design is a permanent magnet,

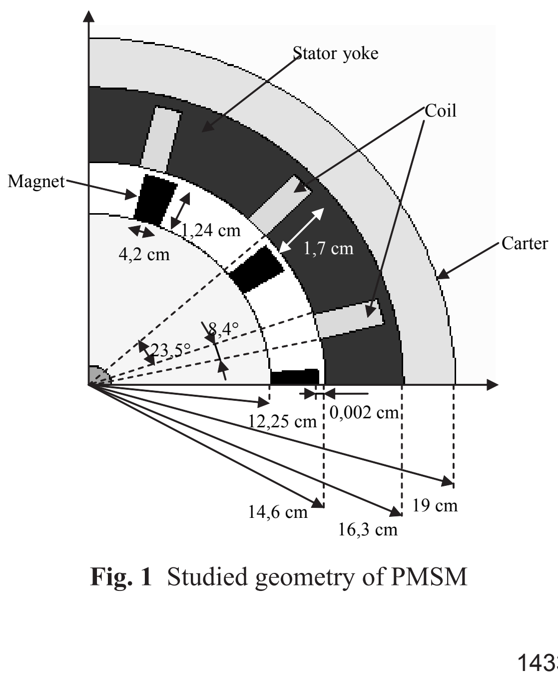

Fig. 1 Studied geometry of PMSM

concentrated winding, opened slot, radial flux and sinusoidal wave-form [Tounsi et al., 2004; Neji et al., 2005]. This sinusoidal wave-form is characterized by pairs pole number ($p = 5$).

The phase resistance R is given by the formula:

$$R = \rho \frac{N_{sph} L_{sph}}{S_c} \quad (1)$$

Different operating losses generated in various regions are calculated accordingly and form heat sources in the thermal analysis. Copper losses are a function of temperature as the winding resistance is temperature dependent [Tounsi et al., 2003].

The slot height is given by the formula:

$$h_s = \sqrt{\frac{2 I_p N_{sph}}{\sqrt{2} N_t \delta K_{fu} A_{ws}} + \left(R_m + \frac{g}{2}\right)^2} - \left(R_m + \frac{g}{2}\right)^2 \quad (2)$$

The weight of stator yoke W_{sy} and teeth W_t are given by respectively:

$$W_t = \frac{A_{wt}}{2} N_t \left[\left(R_m + \frac{g}{2} + h_s\right)^2 - \left(R_m + \frac{g}{2}\right)^2\right] l_m d \quad (3)$$

$$W_{sy} = \pi \left[\left(R_m + \frac{g}{2} + h_s + t_{sy}\right)^2 - \left(R_m + \frac{g}{2} + h_s\right)^2\right] l_m d \quad (4)$$

The weight of rotor yoke is obtained by formula:

$$W_{ry} = \pi \left[\left(R_m - \frac{g}{2} - t_m\right)^2 - \left(R_m - \frac{g}{2} - t_m - t_{ry}\right)^2\right] l_m d \quad (5)$$

The weight of the copper is:

$$W_c = 3\left[2 l_m + 4 A_{ws}\left(R_m + \frac{g}{2} + \frac{h_s}{2}\right)\right] N_{sph} \left(\frac{I_p}{\delta\sqrt{2}}\right) d_c \quad (6)$$

The weight of the magnet is:

$$W_m = \frac{W_m}{2}\left[\left(R_m - \frac{g}{2}\right)^2 - \left(R_m - \frac{g}{2} - t_m\right)^2\right] l_m 2 p\, d_m \quad (7)$$

3. LUMPED-CIRCUIT ANALYSIS

The thermal model is based upon lumped-circuit analysis. It represents the thermal problems by using the thermal networks, analogous to electrical circuits. The thermal circuit in the steady state consists of thermal resistances and heat sources connected between motor component nodes [Chin et al., 2003; Staton et al., 2003; Staton et al., 2001; André et al., 2007; Wen et al., 2007].

For transient analysis, the heat/thermal capacitances are used additionally to take into account the change in internal energy of the body with time. Thermal resistances for conduction and convection can be obtained by formula [Boglietti et al., 2009]:

$$R_{condu} = \frac{l}{Ak} \qquad (K/W) \quad (8)$$

$$R_{conve} = \frac{1}{A_c h} \qquad (K/W) \quad (9)$$

The heat capacitance is defined as:

$$C = V \rho\, c \qquad (Ws/K) \quad (10)$$

Figure 2 presents the schematic diagram of a transient state thermal network of a PMSM.

As described earlier, the thermal resistance values are automatically calculated from motor dimensions and material data. The accuracy of the calculation is dependent on knowledge of the various thermal contact resistances between components within the motor, e.g. slot-liner to lamination and lamination to housing interface.

Figure 3 shows a simplified stator for the thermal study. The thermal resistances are calculated along the radial direction. The R_i radius are calculated from dimensions of motor.

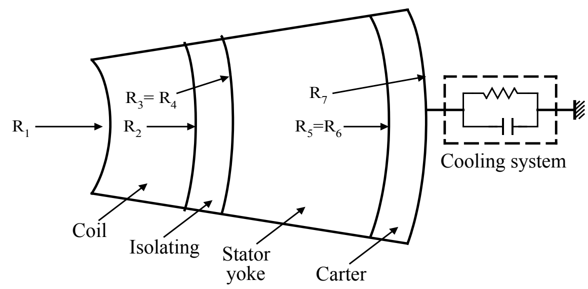

Fig. 3 Simplified stator for the thermal study

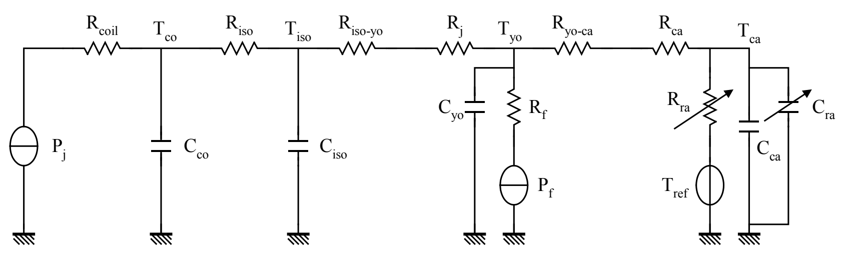

Fig. 2 Thermal model simplified of the motor

With:

$$
\begin{aligned}
&R_1 = R_m\\
&R_2 = R_1 + hs\\
&R_3 = R_2 + 0.003\\
&R_4 = R_3\\
&R_5 = R_4 + tsy\\
&R_6 = R_5\\
&R_7 = R_6 + 0.01
\end{aligned}
\tag{11}
$$

The sources of heat in this model correspond respectively to the copper losses (P_j) and iron losses (P_f) in the stator. The variables T_i correspond to the temperatures in various points of the motor. The expressions of thermal resistances result from the resolution of the equation of heat at the borders of the fields.

R_{coil}: represents the coil thermal resistance (K/W). This resistance is given by following equation:

$$R_{coil} = \frac{1}{4\pi l_m \lambda_c}\left[1-2\left(\frac{R_1}{R_2^2-R_1^2}\right)\ln\frac{R_2}{R_1}\right] \tag{12}$$

The isolating thermal resistance (R_{iso}) is given by following equation (K/W):

$$R_{iso} = \frac{\ln\left(\frac{R_3}{R_2}\right)}{2\pi l_m \lambda_i} \tag{13}$$

The thermal resistance of contact between isolating and stator yoke ($R_{iso\text{-}yo}$) is given by (K/W):

$$R_{iso-yo} = \frac{r_1}{2\pi l_m R_3} \tag{14}$$

R_j: Thermal resistance of stator yoke (K/W), is given by formula:

$$R_j = \frac{\ln\left(\frac{R_5}{R_4}\right)}{2\pi l_m \lambda_{yo}} \tag{15}$$

R_f: represents the isolating thermal represent the thermal resistance of conduction of heat in the iron yoke (K/W), is given by:

$$R_f = \frac{1}{4\pi l_m \lambda_{yo}}\left[1-2\left(\frac{R_4}{R_5^2-R_4^2}\right)\ln\frac{R_5}{R_4}\right] \tag{16}$$

$R_{yo\text{-}ca}$: represents the thermal resistance between stator yoke and the carter (K/W). This resistance is given by following equation:

$$R_{yo-ca} = \frac{r_2}{2\pi l_m R_5} \tag{17}$$

R_{ca}: represent the thermal resistance of carter (K/W). This resistance is given by following equation:

$$R_{ca} = \frac{\ln\left(\frac{R_7}{R_6}\right)}{2\pi l_m \lambda_{ca}} \tag{18}$$

The expressions of the heat capacities are given by:

- Heat capacity of coil (J.K^{-1}).

$$C_{co} = \frac{W_c C_{pco}}{N_{sl}} \tag{19}$$

- Heat capacity of isolating (J.K^{-1}).

$$C_{iso} = \frac{\rho_{iso} V_{iso} C_{piso}}{2N_{sl}} \tag{20}$$

- Heat capacity of stator yoke (J.K^{-1}).

$$C_{yo} = \frac{W_{sy} C_{pf}}{2N_{sl}} \tag{21}$$

- Heat carter capacity (J.K^{-1}).

$$C_{ca} = \frac{\rho_{al} C_{al} 2\pi l_m \left(R_7^2 - R_6^2\right)}{2N_{sl}} \tag{22}$$

R_{ra} and C_{rd}: thermal resistance and capacity of the cooling system respectively.

4. MACHINE MODEL IN MOTOR-CAD

Motor-CAD is a commercial software package dedicated to the optimization of motor cooling. Its solver is based on thermal lumped circuit analysis. This provides near instantaneous calculations speeds allowing 'what-if' scenarios to be run in real time. The user inputs geometric data for the design they wish to simulate using the graphical radial and cross-section editors.

The motor PMSM represented in Figure 1 is implemented in the Motor-CAD software [Motor-CAD v3.1, 2006]. The cross-section and axial views in Motor-CAD are shown in Figures 4 and 5.

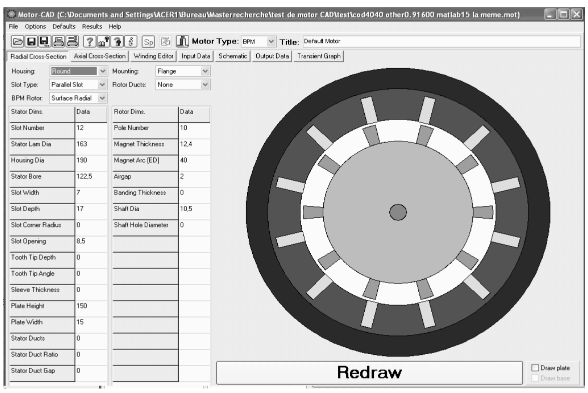

Fig. 4 Cross-section showing fining from Motor-CAD

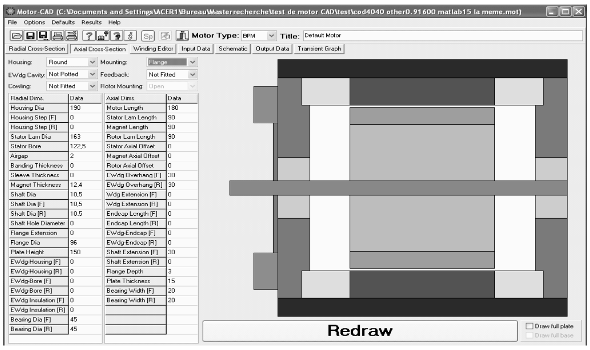

Fig. 5 Axial section

5. RESULTS AND DISCUSSION

The thermal model shown in Figure 2 is implemented in MATLAB simulator [MATLAB, 2002] in order to estimate the different temperatures at any part of the motor.

In order to shows the good accuracy of the proposed model, simulations by Motor-CAD software are performed in static and dynamic conditions.

5.1 Static behaviour of the proposed thermal model

Figure 6 show the evolution of the coil temperature and stator yoke temperature in the motor as a function of the copper losses and the iron losses injected in the motor. The ambient temperature is fixed at 40 degrees Celsius. These results are obtained by the motor-CAD and by the proposed model.

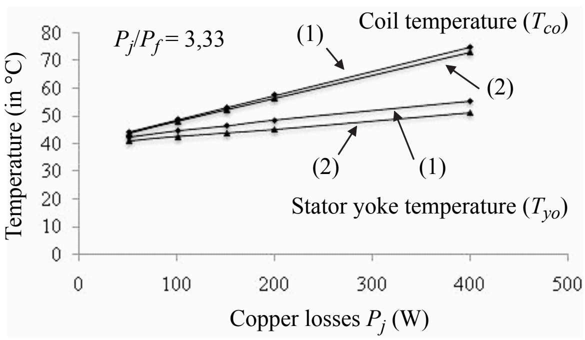

Fig. 6 Evolution of the coil temperature and stator yoke temperature in the motor as a function of copper losses injected in the motor (ambient air = 40 °C)
((1): obtained by thermal model and (2): obtained by motor-CAD)

Figure 7 shows the evolution of the coil temperature and stator yoke temperature in the motor as a function of the conditions cooling system (R_{rd}).

A good accuracy is noted between the different results, this implies that the thermal model is an accurate model for static thermal analysis.

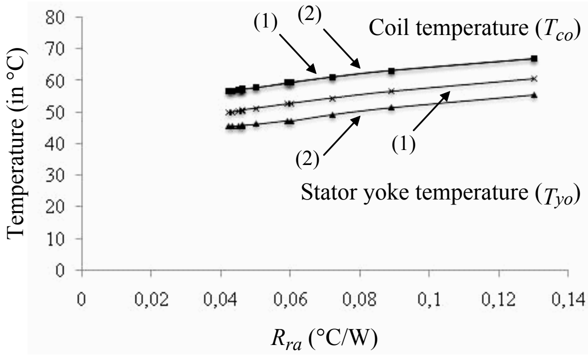

Fig. 7 Evolution of the coil temperature and stator yoke temperature in the motor as a function of R_{ra} (ambient air = 40 °C, P_j = 200 W and P_f = 60W)
((1): obtained by thermal model and (2): obtained by motor-CAD)

5.2 Transient analysis

To verify the accuracy of the thermal model in the transient state, copper losses and the iron losses injected in the motor

Figure 8 shows the transient thermal responses at the coil temperature and stator yoke temperature in the motor when copper losses and the iron losses is equal to 200 W and 60 W respectively. These results are obtained by the thermal model proposed and the motor-CAD software considered as a reference.

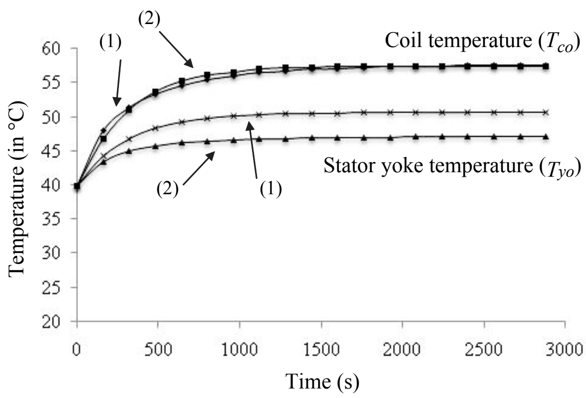

Fig. 8 Evolutions of the coil temperature and stator yoke temperature
((1): obtained by thermal model and (2): obtained by motor-CAD) (P_j = 200 W, P_f = 60 W and R_{ra} = 0.045 K/W)

Figure 9 shows the transient thermal responses at the coil temperature, stator yoke temperature and carter temperature in the motor when copper losses and the iron losses is equal to 500 W and 100 W respectively. These results are obtained by the thermal model proposed and the motor-CAD software considered as a reference.

A good accuracy is noticed between the thermal model and the results obtained by motor-CAD software.

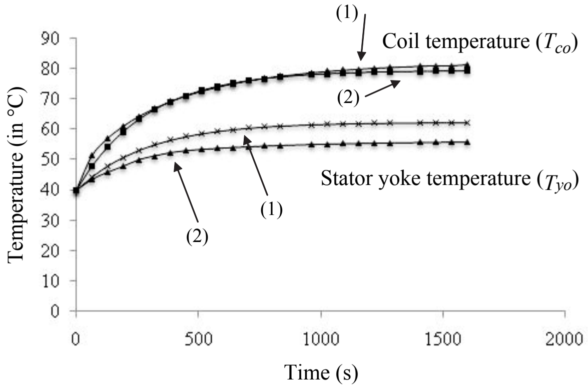

Fig. 9 Evolutions of the coil temperature and stator yoke temperature
((1): obtained by thermal model and (2): obtained by motor-CAD) (P_j = 500 W, P_f = 100 W and R_{ra} = 0.04 K/W)

So, transient thermal behavior of the proposed model is correct and the introduced error is not important.
We notice that the simulation cost of the proposed thermal model is very small compared to the simulation cost of the motor-CAD. A CPU-cost ratio of (10^4) is registered between the two simulations when they are performed with a Pentium processor.

5.3 Thermal behavior of the motor in the case of pulsed losses

Some recent technological approaches in traction application are of interest. With a growing awareness of electronic and acoustic noise in the consumer environment, manufacturers are beginning to raise the operating frequency of devices from a few KHz to above 10 KHz.
The duty factor is a fraction of the cycle period spent at peak power, $\alpha = \frac{t_{on}}{T}$ and the frequency as the inverse the cycle period time $f = \frac{1}{T}$. To predict the pulse operation characteristics, these definition are used as shown in Figure 10.

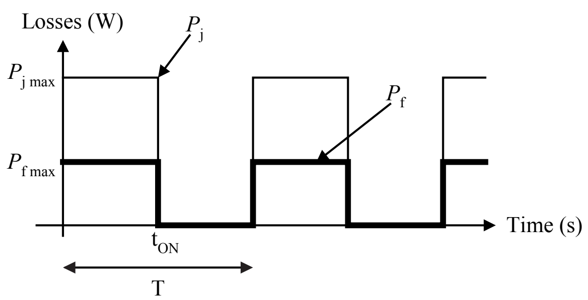

Fig. 10 The waveform sketch of pulsed power losses injected in the motor

Figure 11 shows the transient thermal coil (T_{co}) temperature evolution obtained by the advanced model and by the Motor-CAD. These results are obtained by applying the pulse train sketched in Figure 10.

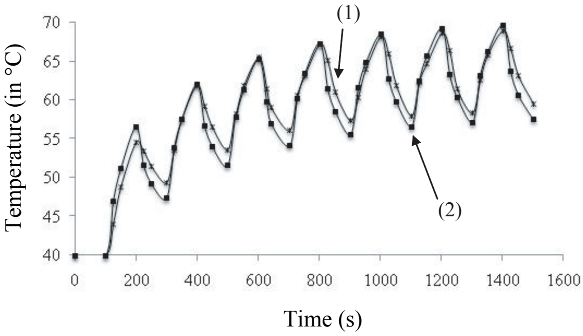

Fig. 11 Transient thermal coil (T_{co}) temperature evolution
((1): obtained by thermal model and (2): obtained by motor-CAD) (P_{jmax} = 600 W, P_{fmax} =180 W, a = 0,5 and R_{ra} = 0.04 K/W)

A good accuracy is noticed between the thermal model and the Motor-CAD simulations. So, transient thermal behavior of the proposed model is correct and the introduced error is not important. We notice that the simulation cost of the proposed thermal model is very small compared to the simulation cost of the motor-CAD. A CPU-cost ratio of (10^4) is registered between the two simulations when they are performed with a Pentium processor.
The motor is running at a repeated operation periods. Each period consist of one part with constant power. The operation period is much shorter that the thermal equilibrium is not reached. The copper losses and the iron losses are injected into the thermal model is show in Figure 12. Figure 13 shows the transient thermal coil (T_{co}) temperature evolution and the transient thermal stator yoke (T_{yo}) temperature evolution obtained by the advanced model.

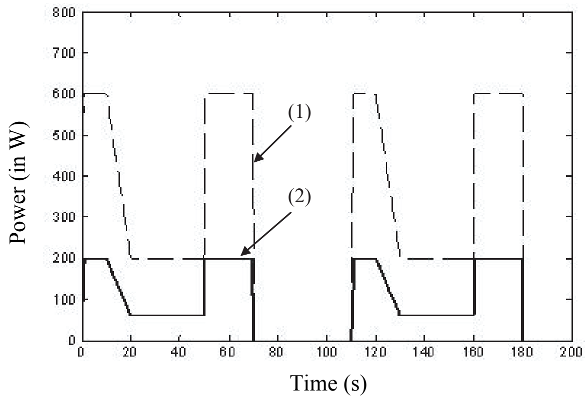

Fig. 12 Copper losses (1) and iron losses injected (2) into the thermal model

5.4 Thermal behavior of the motor in the case of mission circulation

For intermittent operation a mission of circulation is

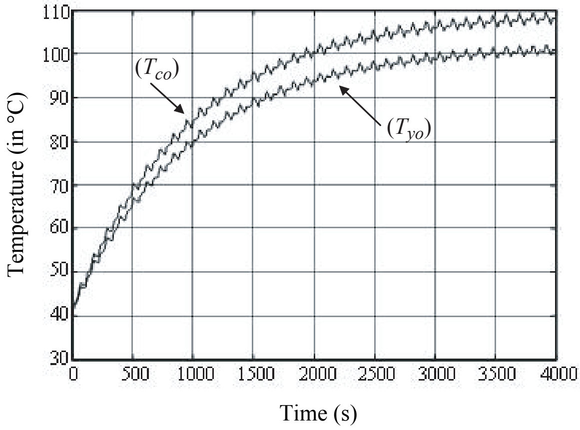

Fig. 13 Transient thermal coil (T_{co}) and thermal stator yoke (T_{yo}) temperature evolution (R_{ra} = 1K/W)

used. The Figures 14 and 15 illustrate the losses in the channel of traction on a mission of circulation. The copper losses and the irons losses are injected into the thermal model. Figure 16 shows the results simulated during repeating operation periods.

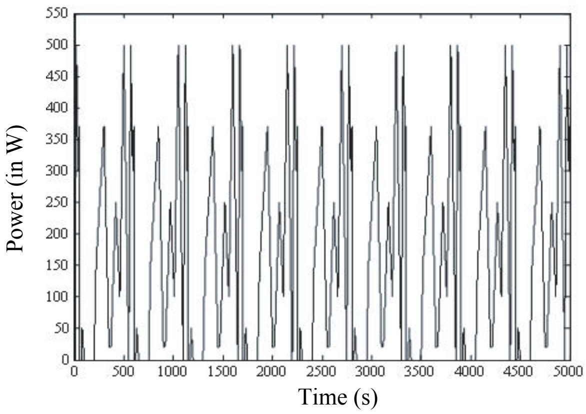

Fig. 14 Copper losses injected in the thermal model

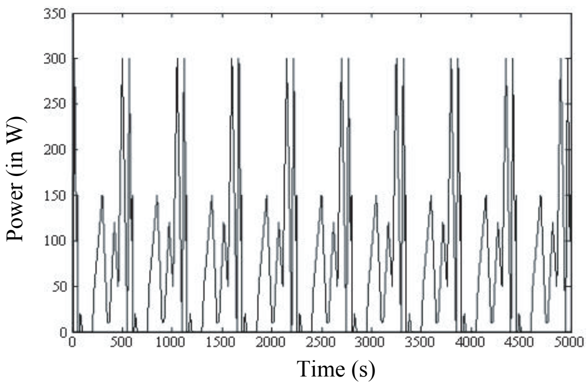

Fig. 15 Irons losses injected in the thermal model

6. CONCLUSION

The thermal analysis of permanent magnet synchronous motor is presented. The lumped circuit approach is employed in this investigation. The proposed model is compatible with circuit simulators.

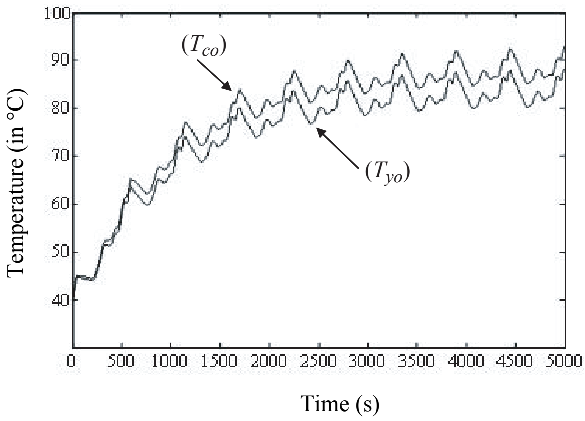

Fig. 16 Transient thermal coil (T_{co}) and thermal stator yoke (T_{yo}) temperature evolution (R_{ra} = 1 K/W)

Simulations by Motor-CAD software performed in order to study the variations of the temperature at any part of the motor, according to the copper losses and the iron losses injected in the motor and the boundary conditions at the cooling systems. We not, that this method can be applied to all other type of motor.

We notice that the simulation cost of the proposed thermal model is very small compared to the simulation cost of the motor-CAD. A CPU-cost ratio of (10^4) is registered between the two simulations when they are performed with a Pentium processor.

References

André, M. S., X. M. López-Fernández, and A. J. Marques Cardoso, Thermal behavior of a three-phase induction motor fed by a fault-tolerant voltage source inverter, *IEEE Transaction on Industry Applications*, Vol. 43, No. 3, 724-730, 2007.

Boglietti, A., A. Cavagnino, and C. Mejuto, Evolution and modern approaches for thermal analysis of electrical machines, *IEEE Transactions on Industrial Electronics*, Vol. 56, No. 3, 871-882, 2009.

Chin, Y. K., E. Nordlund, and E. A Staton, Thermal analysis: Lumped circuit model and finite element analysis, *Proceesings of Sixth International Power Engineering Conference*, 952, 2003.

Chaieb, M., N. B. Hadj, J. K. Kammoun, and R. Neji, A comparative study of tow permanent magnet motor structures with interior and exterior rotor, *Journal of Asian Electric Vehicles*, Vol. 8, No. 1, 1363-1370, 2010.

Fakhfakh, M. A., M. H. Kasem, S. Tounsi, and R. Neji, Thermal analysis of a permanent magnet synchronous motor for electric vehicles, *Journal of Asian Electric Vehicles*, Vol. 6, No. 2, 1145-1151, 2008.

Motor-CAD v3.1, software manual, 2006.
MATLAB, MATLAB 6p5 Simulator Data Book, 2002.
Neji, R., S. Tounsi, and F. Sellami, Optimization and design for a radial flux permanent magnet motor for electric vehicle, *Journal of Electrical Systems*, Vol. 1, No. 4, 47-68, 2005.
Staton, D. A., A. Boglietti, and A. Cavagnino, Solving the more difficult aspects of electric motor thermal analysis, Proceesings of IEEE IEMDC, 47-55, 2003.
Staton, D. A., Thermal computer aided design: Advancing the revolution in compact motors, Proceedings of IEEE IEMDC, 858, 2001.
Tounsi, S., R. Neji, and F. Sellami, Modélisation des pertes dans la chaîne de traction du véhicule electrique, Proceedings of CTGE, 291-297, 2004.
Tounsi, S., R. Neji, F. Sellami, Design of a radial flux permanent magnet motor for electric vehicle, Proceeding of EPE, CD-Rom, 2003.
Wen, X., W. Hu1, T. Fan, and J. Liu, Lifetime model research of motor drive system for electric vehicles, Proceedings of International Conference on Electrical Machines and Systems, 129-132, 2007.

(Received October 8, 2010; accepted December 18, 2010)

Appendix

Nomenclature:
ρ: Density
N_{sph}: Number of spire per phase
L_{sph}: Length of spire per phase
S_c : Copper area
I_p: Pick current feeding the motor
K_{fu}: Coefficient of filling slot
D_c: Density of the copper
N_t: Number of teeth
δ: Current density
A_{ws}: Slot angular width
R_m: Bore radius
g: Air-gap thickness
A_{wt}: Tooth angular width
l_m: Motor length
d: Density of the metal sheet
T_{sy}: Stator yoke height
t_m: Magnet height
t_{ry}: Rotor yoke height
d_m: Density of magnet
λ_c: Copper thermal conductivity
λ_t: Isolation thermal conductivity
r_1: Thermal resistance of surface contact between isolating material and stator yoke
λ_{yo}: Iron thermal conductivity
r_2: Thermal resistance of surface contact between stator yoke and carter
λ_{ca}: Carter thermal conductivity
C_{pco}: Copper massive heat capacity
N_{sl}: Number total of spire
ρ_{iso}: Isolating density
V_{iso}: Isolating volume
C_{piso}: Isolating massive heat capacity
C_{pf}: Iron massive heat capacity
ρ_{al}: Aluminum density
C_a: Aluminum massive heat capacity
l: Distance between the point masses
A: Interface area
k: Heat conductivity
A_c: Cooling cross section
h: Convection coefficient
V: Material volume
c: Heat capacity of the material